# 論文 The Seismic Behavior of Precast Columns using High-Strength Concrete subjected under High Axial Loading

Primo Allan ALCANTARA[*1], Juan Jose CASTRO[*2], Teruaki YAMAGUCHI[*2] and Hiroshi IMAI[*3]

**ABSTRACT:** This research focuses on the results of the latest experiment done regarding the structural performance of precast concrete columns constructed using the main bar post-insertion system. Here, its main objective is to determine the influence of the use of high-strength concrete to the seismic behavior of precast concrete columns when subjected under high axial loading. Also, an analysis on the shear and bond splitting capacities of the columns would be done.
**KEYWORDS:** precast concrete column, high-strength concrete, axial loading, shear capacity, bond splitting capacity

## 1. RESEARCH BACKGROUND

This research is the latest on the series of experiments dealing with the application of the main bar post-insertion method [1] to precast concrete columns. This system features the use of spiral steel sheaths which are hollow tubes positioned in place of the main bars in precast concrete members wherein such bars are to be later inserted during assembly. The first on the series [2] dealt with a different type of casting method called centrifugation. The second and the third [3,4] features the ordinary casting of concrete with investigation of the influence of varying the amount of lateral reinforcement. Here, normal-strength concrete (30 MPa) was used and two levels of axial loading were applied ($0.1\sim0.2F_c$). Also, in evaluating the structural performance of the main bar post-insertion method, the use of lapping joints at midheight were implemented. Lastly, the fourth [5] considers the effect of varying the yield strength of the lateral reinforcement and in order to fully assess the performance of the spiral steel sheaths, continuous main bars were used.

For this series, the use of high-strength concrete (70 MPa) and the application of a high level of axial loading ($0.3\sigma_B$) are the main considerations. Here, both the bond splitting and shear capacities of the columns would be investigated. Also, to evaluate the seismic performance of the precast columns using the aforementioned method, additional monolithic specimens were tested.

## 2. SPECIMEN DETAILS

A total of 10 specimens were constructed consisting of 8 precast concrete and 2 monolithic types. Table 1 shows the specimen specifications while Fig. 1 gives a layout of the columns. The specimens tested were grouped into two types; first, columns casted with normal-strength concrete

*1 Graduate School, University of Tsukuba, Member of JCI
*2 Technical Research Institute, Kabuki Construction Co. Ltd., Member of JCI
*3 Institute of Engineering Mechanics, University of Tsukuba, Member of JCI

($F_c$=30MPa), and second, those with high-strength concrete ($F_c$=50MPa). Main variations lie on the amount of lateral reinforcement as characterized by the differences in the number of lateral ties and spacing of the hoops. Here, very high axial loading is applied representative of first storey columns of high-rise structures of more than 15 floors. Also, for this series, continuous main bars were again adapted to further evaluate the performance of the sheaths. In addition, to compare the bond performance of top and bottom-cast bars, the concrete was cast in the direction of the applied shear loading, thereby making the extreme rows of main reinforcement as top and bottom-cast main bars.

**Table 1 Column Specifications**

| Specimen PCa | Specimen RC | Lateral Reinforcement Bar Arrangement | Lateral Reinforcement Ratio $p_w$ (%) | Design Concrete Strength $F_c$ (MPa) | Axial Load (kN) |
|---|---|---|---|---|---|
| C61P | C61M | 4-D10@150 | 0.42 | | |
| C62P | - | 6-D10@120 | 0.79 | 30 | 2350 |
| C63P | - | 6-D10@80 | 1.19 | | |
| C64P | - | 4-D10@150 | 0.42 | | |
| C65P | - | 2-D10@75 | 0.42 | | |
| C66P | - | 6-D10@120 | 0.79 | 50 | 3240 |
| C67P | - | 4-D10@80 | 0.79 | | |
| C68P | C68M | 6-D10@80 | 1.19 | | |

Common: b x D x h : 45cm x 45cm x 135cm
main bars : 20-UHD22 (SHD685)
lateral reinforcement : D10 (SD295A)
design grout strength : 60 MPa
Sheath: diameter 34 mm, lug height 2 mm, pitch 28 mm

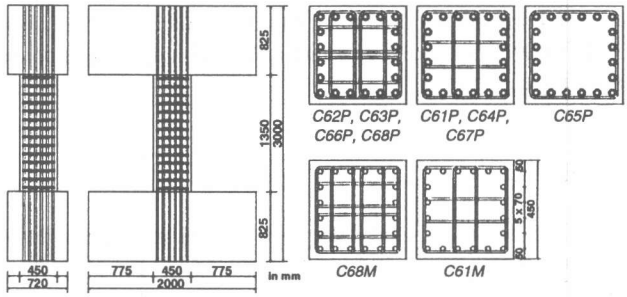


**Fig. 1 Column Specimen**

## 3. LOADING METHOD

Each of the column specimens was set under the loading apparatus shown in Fig. 2. These specimens were subjected to varying shear forces that were applied in a cyclic manner producing anti-symmetric bending moment distribution while being acted upon by a high constant axial load. Each specimen was set using oil jacks attached on both sides of the upper and lower loading beams. Here, the shear force was applied through the horizontal actuator while the axial load was provided by the four vertical actuators shown. For the proper simulation of seismic behavior, each specimen was made to drift once at a drift angle R equal to ± 1/800, then twice at R of ± 1/400, ± 1/200, ± 1/100 and ± 1/50 and again once at R equal to ± 1/25. To follow the prescribed loading history, displacement transducers were installed on both sides of the specimen. Along the height of the column, clip gauges were systematically arranged to measure local deformation. Asides from these, strain gauges were strategically positioned all over the reinforcing bars of the specimen.

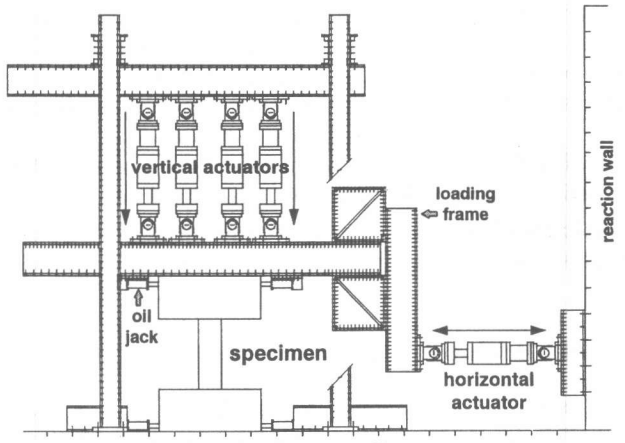


**Fig. 2 Loading System**

## 4. MATERIAL TEST RESULTS

Table 2 shows the material properties of the reinforcing bars and concrete used in the experiment. In actual design practice, ordinary strength bars are used for the main reinforcement, but for experimental purposes, high strength bars were used. As for the concrete, results show that higher strengths, as compared to their specified values, could be observed for both the normal and high-strength concrete types.

**Table 2 Material Test Results**

(a) Reinforcing Bars (MPa)

| Size | Grade | Young's Modulus | Yield Strength | Tensile Strength | Elongation % | Type |
|---|---|---|---|---|---|---|
| D22 | SHD685 | $1.87 \times 10^5$ | 677 | 899 | 8.9 | Main |
| D10 | SD295A | $1.94 \times 10^5$ | 377 | 514 | 14.9 | Hoop |

(b) Concrete (MPa)

| Specimen | Compressive Strength | | Split |
|---|---|---|---|
| | 28 days | at the time of testing | Strength |
| C61M | 24.5 | 38.7 | 3.6 |
| C61P, C62P & C63P | 24.3 | 36.9 | 3.0 |
| C64P, C65P & C66P | 58.3 | 69.4 | 4.2 |
| C67P, C68P & C68M | 58.3 | 70.4 | 4.5 |

## 5 EXPERIMENTAL RESULTS

### 5.1 CRACK PATTERNS

The progress of the experiment could be described using the observed cracks patterns. In general, initial cracking on the critical section at the column end occurred during the first cycle at R=1/800 for all specimens. For the normal-strength concrete specimens (C61M~C63P), it was observed that the concrete stress exceeded its tensile strength due to the presence of flexural cracks at the end portions of the columns at R=1/400. For the high-strength concrete specimens (C64P~C68M), this occurred at R=1/200. Also, it was during this cycle that extensions of the flexural cracks as well as the appearance of the initial shear cracks were observed for all specimens. However, more shear cracks could be seen for the normal-strength concrete specimens wherein it covered the whole height of the column. A typical sample on the crack behavior is shown in Fig. 3.

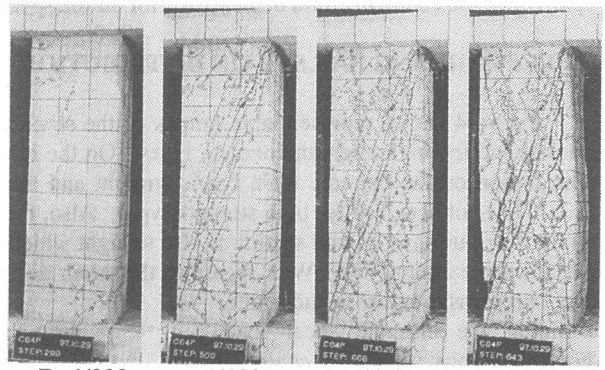

R=1/200 1/100 1/50 1/25

**Fig. 3 Crack Patterns (C64P)**

The next discussion focuses on the crack behavior of the normal-strength concrete columns (C61M~C63P) during the latter half of the experimentation. Except for C61M, further propagation of the shear cracks was observed at R=1/100. And as for C61M, it was during this cycle that bond splitting cracks commenced concentrating on the area along the row of the top-cast main reinforcement. This is naturally the case since the calculated bond strength of the top-cast bars is lower than the bottom-cast bars. Also, it was during this cycle that specimens C61M and C61P reached their ultimate strengths. Based on the observed crack patterns, it could be said that C61M failed in bond splitting while C61P in shear. Continuing, at R=1/50, the precast specimens exhibited widening of the shear cracks as well as spalling of the concrete cover. On the other hand, the monolithic specimen showed further widening of the bond splitting cracks. However, for specimens C62P and C63P, it was observed that asides from the shear cracking, prominent bond splitting cracks could be seen along the row of the top-cast bars. Also, it was during this cycle that they attained their ultimate strengths. Therefore, the failure mode of specimens C62P and C63P could be judged as of lying on an area in between the shear and bond splitting types based on the crack pattern at peak loading.

The remaining discussion would now focus on the high-strength concrete columns (C64P~C68M). At R=1/100, propagation of shear cracks along the whole height could be observed for the specimens. A major observation that could be seen here lies on the specimens having the same amount of lateral reinforcement (C64P-C65P and C66P-C67P) but differing in the number of lateral ties. From Table 1, it could be seen that C64P and C66P have a greater number of lateral ties than C65P and C67P, respectively. For specimens C65P and C67P as well as C68M, along with the occurrence of shear cracks is the presence of prominent bond splitting cracks on the area of the top-cast bars. At this cycle, specimens C64P and C65P attained ultimate strength. C64P failed in shear as evidenced by the emphasized shear cracking along the main diagonal while C65P failed in either shear or bond splitting due to the presence of both types of cracks at failure. Continuing, cycle R=1/50 saw the appearance of more cracks as well as the widening of the shear cracks. Here, the rest of the specimens reached maximum loading. Due to the prominence of the shear cracks at peak loading, specimens C66P and C68P could be said to have failed in shear. Similarly with C65P, specimens C67P and C68M could either have failed in shear or bond splitting. Lastly, at R=1/25, spalling of the concrete could be observed for all the specimens in general.

## 5.2 REINFORCING BAR STRAIN DISTRIBUTION

Figure 4 shows representative graphs of the strain distribution on the main bars for both the normal and the high-strength concrete types. On the left-hand side, it can observed that the strain distribution on the extreme main bar is straight and has not yielded. This suggests that flexural failure has not occurred for both strength types. Also, for the right-hand side, it can be seen that the strain distribution at an end section is also straight which suggests the validity of the plane sections remain plane assumption. With regard to the strain distribution on the lateral hoops, Fig. 5 shows the progress before and after attaining the ultimate shear load. For the graphs shown, it could be observed for specimens C62P and C66P that there is elastic behavior until R=1/200 and that yielding started at R=1/100. For these two specimens, ultimate strength was reached on the cycle of R=1/50. Except for C61M, the same behavior was observed for the rest of the specimens and hence, it could be concluded that all specimens failed either in total shear or a combination of both shear and bond splitting as evidenced by the yielding of the lateral hoops.

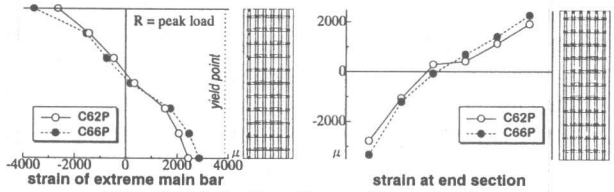


**Fig. 4 Main Bar Strain Distribution**

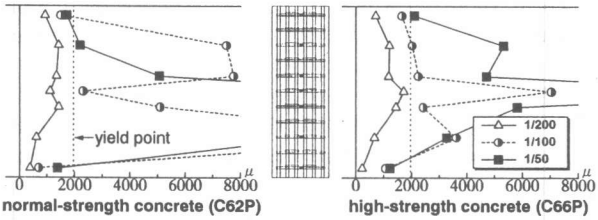


**Fig. 5 Lateral Hoop Strain Distribution**

## 6. ULTIMATE STRENGTH ANALYSIS

Ultimate strength calculations and the experimental results are shown in Table 3. Here, the shear capacity was calculated using the proposed equation (Method A) given in the AIJ's Ultimate Strength Guidelines [6]. On the other hand, the bond splitting capacity was determined using the equation proposed by Kaku [7] wherein the bond strength is calculated using the sheath diameter as the main bar diameter for the precast concrete specimens. Also, in the equation used in the calculation of the bond splitting capacity, the presence of the inner rows of main bars [5] is

considered thereby increasing the effective surface area of the main bars which is very influential in the bond strength. Lastly, the flexural capacity is computed using the proposed equation given in the BCJ's Guidelines [8]. Moreover, the resulting failure mode shown in Table 3 is actually based on the crack behavior during the experimentation as well as on the observed strain distribution on the reinforcing bars.

**Table 3 Ultimate Strength**

| Specimen | $p_w$ (%) | Calculated Values (kN) Shear Capacity | Bond Splitting Capacity | Flexural Capacity | Test Results (kN) | Failure Mode |
|---|---|---|---|---|---|---|
| C61M | 0.42 | 689 | 747 | 1580 | 770 | Bo → S |
| C61P | 0.42 | 681 | 788 | 1569 | 853 | S → Bo |
| C62P | 0.79 | 1005 | 1335 | 1569 | 1033 | S/Bo |
| C63P | 1.19 | 1265 | 1488 | 1569 | 1333 | S/Bo |
| C64P | 0.42 | 765 | 832 | 1861 | 1081 | S → Bo |
| C65P | 0.42 | 766 | 805 | 1861 | 1008 | S/Bo |
| C66P | 0.79 | 1090 | 1469 | 1861 | 1347 | S → Bo |
| C67P | 0.79 | 1089 | 1381 | 1865 | 1301 | S/Bo |
| C68P | 1.19 | 1437 | 1891 | 1865 | 1618 | S → Bo |
| C68M | 1.19 | 1437 | 1891 | 1865 | 1611 | S/Bo |

Bo : bond splitting  S : shear  → : subsequent occurrence  / : coincident occurrence

## 6.1 BOND SPLITTING CAPACITY

For this series, it is generally very hard to clearly classify the resulting failure mode as either shear or bond splitting due to the presence of both types of cracks at failure. However, by also observing the strain distribution of the reinforcing bars and the prominence of both types of crack patterns, a close evaluation on the resulting failure mode can be done as shown in Table 3. Among the main conclusions that could be derived with regard to the bond splitting capacity are the following. First, considering specimens C61M and C61P, since their design specifications are the same, it is expected that they fail in a similar manner. However, results show that C61M failed in bond splitting while C61P failed in shear. This proves that the bond splitting capacity of precast concrete columns are generally higher than their monolithic counterparts. This behavior could also be seen for specimens C68P and C68M wherein the latter shows very prominent bond splitting cracks at failure. Secondly, considering the influence of the number of tie legs on the bond splitting capacity, focus would be given on specimens C64P~C67P. Calculations show that there is no effect on the shear capacity but there is a slight decrease on the bond splitting capacity for lesser number of lateral ties having the same amount of lateral reinforcement. Such behavior was observed when comparing specimen C64P (4 ties) with C65P (2 ties). Specimen C65P showed more prominent bond splitting cracks at failure and also a slightly lower ultimate strength. This behavior was also shown by specimens C66P (6 ties) and C67P (4 ties). Therefore, it could be said that a decrease on the number of lateral ties at a constant $p_w$ decreases the bond splitting capacity of columns. Lastly, with regard to the bond behavior of top-cast bars as compared to bottom-cast bars, it was observed that, specially for specimens C62P, C65P and C67P, the appearance of bond splitting cracks is much more emphasized on the area of the top-cast bars. Such a result is in agreement with the findings reported by Yanez [9] with regard to the bond strength of spiral steel sheaths as influenced by the location of the bars during casting.

## 6.2 SHEAR CAPACITY

As for the analysis on the shear capacity, emphasis would be given on the specimens failing in shear. From Table 3, it could be observed that the calculated shear capacity is a little underestimated for both the normal and high-strength concrete types. The same behavior is also shown in Fig. 6. Previous discussions presented in reference [3] suggests that such discrepancy could be attributed to an effect of the applied axial loading on the shear capacity of columns. This

would be further verified for higher ratios of axial loading and higher concrete strength columns. Figure 6 represents the ultimate strength results of the experiment. The dotted line represents the proposed adjustment on the shear capacity of columns and is given by eq. (1).

$$V_u = bj_t p_w \sigma_{wy} \cot\phi + \tan\theta(1-\beta)bD\nu\sigma_B / 2 + 0.1\sigma_o bj_t \qquad (1)$$

where $\sigma_o$ : axial compressive stress, $b, D$ : width and overall depth of the column, $j_t$ : distance between extreme rows of main bars, $p_w$ : lateral reinforcement ratio, $\sigma_{wy}$ : yield strength of lateral reinforcement, $\phi$ : compressive strut angle in the truss mechanism, $\theta$ : compressive strut angle in the arch mechanism, $\beta$ : proportion of concrete stress carried by the truss mechanism, $\nu$ : concrete strength effectiveness factor, $\sigma_B$ : concrete compressive strength

The only difference with the AIJ shear equation could be seen on the additional third term which expresses the effect of axial loading. Quantitatively, it is one-tenth of the applied axial compressive stress multiplied by the column width and the distance between the outer main reinforcement. Experimental results show a fairly good agreement with the adjusted shear capacity for those having a high ratio of axial loading ($0.3\sigma_B$) as shown on the left-hand graph of Fig. 6. Also, such adjustment could be applied for higher-strength concrete columns (70 MPa) shown on the right-hand graph of Fig. 6.

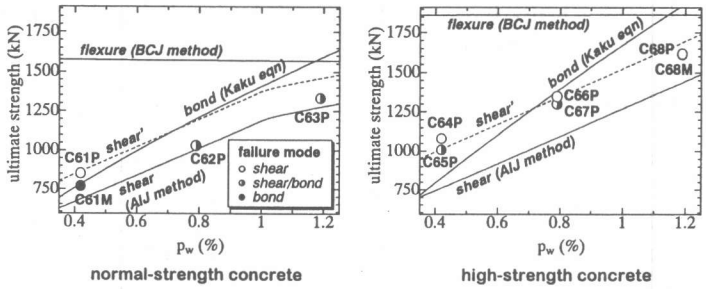


**Fig. 6 Ultimate Strength**

## 7. CONCLUSIONS

a) The proposed adjustment on the shear capacity equation could be applied to columns subjected to high axial loading as well as to those using high-strength concrete.
b) At a constant amount of lateral reinforcement ($p_w$), a decrease in the number of lateral ties decreases the bond splitting capacity of the columns.
c) The bond strength of top-cast bars is lower than that of bottom-cast bars in precast columns.
d) The seismic performance of precast concrete columns using the main bar post-insertion system is generally similar to their monolithic counterparts.

## REFERENCES


1. Imai, H., "Precast Method for Frame Type Buildings", Structural Failure Durability and Retrofitting, 1993, pp. 396-403.
2. Kobayashi, T., Yamaguchi, T., and Imai, H., "Shear Performance of Centrifuged Precast Columns with Lapping Joints", Transactions of the JCI, Vol. 13, 1991, pp. 589-596.
3. Kobayashi, T., et al., "An Experimental Study on the Seismic Performance of Precast Concrete Columns under Shear Forces", Transactions of the JCI, Vol. 14, 1992, pp. 409-416.
4. Alcantara, P.A., et al., "A Study on the Influence of Shear Reinforcement Ratios of the Seismic Performance of Precast Concrete Columns", Transactions of the JCI, Vol. 17, 1995, pp. 173-180.
5. Alcantara, P.A., et al., "A Research on the Seismic Behavior of Precast Concrete Columns using High-Strength Shear Reinforcement", Proceedings of the JCI, Vol. 19, No. 2, 1997, pp. 963-968.
6. AIJ, "AIJ Structural Design Guidelines for Reinforced Concrete Buildings", JCI, 1994, pp. 77-123.
7. Kaku, T., et al., "The Influence of Yield Stress of Transverse Reinforcement on the Bond Strength of Reinforced Concrete Members", Proceedings of the JCI, Vol. 16, No. 2, 1994, pp. 247-252.
8. BCJ, "Guidelines to Structural Calculation under the Building Standard Law", BCJ, 1991, pp. 229-238.
9. Yanez, R., et al., "Study on the Bond Splitting Strength of Sheaths for a Precast Concrete System", Transactions of AIJ, No. 473, 1995, pp. 137-148.